TISSUE ENGINEERING: Part A
Volume 00, Number 00, 2017

DOI: 10.1089/ten.tea.2017.0290

termis
Tissue Engineering
& Regenerative Medicine
International Society

ORIGINAL ARTICLE

Thymus-Derived Mesenchymal Stem Cells for Tissue Engineering Clinical-Grade Cardiovascular Grafts

Dominga Iacobazzi, PhD,[†] Megan M. Swim, PhD,[†] Ambra Albertario, PhD,
Massimo Caputo, MD,[‡] and Mohamed T. Ghorbel, PhD[‡]

Mesenchymal stem cells (MSCs) are attractive tools for regenerative medicine because of their multi-differentiation potential and immunomodulation capacity. In congenital heart defect surgical correction, replacement grafts lacking growth potential are commonly used. Tissue engineering promises to overcome the limitations of these grafts. In this study, we hypothesized that human thymus-derived MSCs are a suitable tool to tissue engineer a living vascular graft with good integration and patency once implanted *in vivo*. Human thymus-derived MSCs (hT-MSCs) were identified by the expression of MSC markers and mesenchymal differentiation potential. When cultured onto natural scaffold to produce tissue-engineered graft, hT-MSCs exhibited great proliferation potential and the ability to secrete their own extracellular matrix. In addition, when implanted *in vivo* in a piglet model of left pulmonary grafting, the engineered graft exhibited good integration within the host tissue, indicating potential suitability for corrective cardiovascular surgery. The optimized xeno-free, good manufacturing practices-compliant culture system proved to be optimum for large-scale expansion of hT-MSCs and production of tissue-engineered cardiovascular grafts, without compromising the quality of cells. This study demonstrated the feasibility of engineering clinical-grade living autologous replacement grafts using hT-MSCs and proved the compatibility of these grafts for *in vivo* implantation in a left pulmonary artery position.

Keywords: tissue engineering, mesenchymal stem cells, GMP grade, thymus, heart, corrective surgery, congenital heart defect

Introduction

Following birth, stem cells reside in tissues for maintenance and repair throughout an individual's lifetime.[1] Among these stem cells are a specific lineage known as mesenchymal stem cells (MSCs). Phenotypic and genetic evidence suggest that MSCs are immature cell types and are able to retain their multilineage differentiation potential *in vitro* until stimulated to the desired phenotype.[2]

To be defined as MSCs, progenitor cells must meet three main criteria: (1) adherence to plastic, (2) specific cell antigen expression, and (3) multipotent differentiation potential to the three main mesenchymal lineages, osteoblasts, adipocytes, and chondroblasts.[3] Most frequently isolated from bone marrow, adipose tissue, and umbilical cord blood, MSCs can also be isolated from a variety of different tissues such as liver, spleen, pancreas, lung, kidney, aorta, vena cava, brain, and muscle.[3]

The perivascular site of the tissue in which they reside has been suggested as the MSC niche.[4] It has also been hypothesized a developmental affiliation between perivascular cells, referred to as pericytes, and MSCs, given that the four surface molecules commonly used as MSC markers CD44, CD73, CD90, and CD105, are natively expressed by pericytes.[5] In particular, Caplan and colleagues have identified pericytes as the source of MSCs, and this easily explains the phenotypical and functional affinity, as well as the same perivascular localization, between the two cell types. In this light, it is a safe assumption to look at MSCs as pericytes; however, all pericytes cannot be regarded as MSCs.[6]

Although cultured pericytes display the same functional behavior of MSCs *in vitro*, recent findings have shown that endogenous pericytes do not exhibit the same plasticity and multilineage capacity as MSCs *in vivo*.[7] Nonetheless, although acting as multipotent progenitor stem cells, the major function of MSCs *in vivo* has been assigned to their capacity to help restore

Bristol Medical School, Bristol Heart Institute, University of Bristol, Bristol, United Kingdom.
[†]Co-first authors.
[‡]Co-senior authors.

and regenerate tissues at the site of injury.[8] Therefore, the perivascular origin of MSCs would adequately justify their role in tissue repair, given that the anatomical location must allow the cells to reach the wounded tissues and organs.

By holding a significant potential in tissue healing and regeneration, supplemental MSCs, either from autologous or allogenic sources, can be provided to help coordinate the tissue regeneration and recovery in a wide range of clinical conditions. In both preclinical and clinical settings, MSCs from different sources have been explored to treat various afflictions, including bone and cartilage diseases,[9–11] graft-versus-host disease,[12] cardiovascular disease,[13–15] liver disease,[16,17] or diabetes mellitus.[18]

Few articles have suggested the neonatal thymus as another potential source of MSCs.[19] The thymus is a central lymphoid organ that is located just above the heart in the upper anterior thorax and is responsible for the maturation of T cells.[20] Reaching its greatest size by the end of the first year of life, the thymus then undergoes involution that continues over the course of an individual's life, becoming largely adipose tissue by the age of 50.[21,22] Its location in neonates, however, means that patients with congenital heart defects (CHD) need a thymectomy before most surgical heart repair. Normally discarded as waste, this tissue is available for cell isolation without needing a donor or taking bone marrow from an already ill child.[23]

The first description of human thymus-derived MSCs (hT-MSCs) was their characterization by differentiation to the three main mesenchymal lineages, as well as to myoblasts.[24] Their multilineage potential has also been demonstrated by the capacity to differentiate to neural-like cells[25] and cardiomyocytes.[26] hT-MSCs have been traced *in vivo* to the interlobular trabeculae of the thymus.[19] One of the main benefits of thymus MSCs is their immune response regulatory ability, thanks to its pivotal role in immune system development and function.[27] When thymus MSCs were cocultured with blood-derived T lymphocytes, the MSCs significantly inhibited the proliferation of the T lymphocytes, thus demonstrating their immune regulation.[27]

Along with these unique therapeutic properties, their ease of accessibility and expansion from discarded thymuses during pediatric open-heart surgeries suggests that hT-MSCs may be a useful therapeutic tool for the treatment of children born with CHD.

Current treatment for CHD by corrective surgery revolves around the use of prosthetic replacement grafts. Graft options currently used include prostheses such as Gore-Tex, allografts, homografts, and xenografts, which are usually porcine or bovine.[28,29] However, these grafts have limited durability and often require repeat operations because of the lack of growth potential.[30,31]

Tissue engineering (TE) has emerged as a novel and promising approach to overcome the limitation of current treatments. By combining the use of autologous MSCs and biocompatible scaffolds, TE promises to create autologous cardiovascular grafts that could potentially remodel, repair, and grow alongside the children's growth. Most of the current protocols for MSC expansion and TE involve the use of animal-derived serum, growth factors, and enzymes for cell isolation and expansion. One of the main challenges for the clinical translation of cell-based tissue engineering therapy is to replace the animal-derived components used for cell isolation and expansion with products to eliminate the risk of graft rejection, immune reactions, and viral or bacterial infections.[32,33] Furthermore, it is compulsory that all the components used throughout the engineering of the graft, as well as the technical procedures, are made according to good manufacturing practices (GMP), to ensure optimal and safest quality in tissue transplantation.[34,35]

In this study, we hypothesized that human thymus-derived MSCs are a suitable tool to tissue engineer a living vascular graft with good patency and integration upon *in vivo* implantation. We have first purified, characterized, and successfully *in vitro* expanded multipotent MSCs from hT-MSCs. In addition, we have optimized the hT-MSC culture and growth onto a naturally occurring scaffold (CorMatrix), on which cells retained their stemness status that is important for the paracrine signals to the surrounding environment and for tissue regeneration. We demonstrated that the produced living tissue provided a good engraftment and lumen endothelialization upon *in vivo* implantation into a large animal model. Furthermore, we have eliminated the use of animal-derived components from isolation throughout the production of the tissue-engineered vascular graft.

To the best of our knowledge, this is the first study comparing the biological and functional properties of hT-MSCs and hT-MSC-derived tissue-engineered vascular graft, cultured in standard and GMP culture systems. The capacity of human thymus-derived MSCs to grow in an animal-free and GMP-compliant environment is an important step for the clinical translation of our hT-MSC TE approach. This study represents the proof of concept that it is possible to produce clinical-grade cardiovascular grafts capable of *in vivo* integration for congenital heart disease corrective surgery.

Materials and Methods

Ethics

Human tissue was collected from patients undergoing congenital heart surgery in compliance with the Human Tissue Act. Perinatal and leftover material (the thymus) was taken with parents' consent under NHS ethics license (REC ref. 06/Q2001/197 and 11/SW/0122).

Isolation and culture of thymus MSCs

Thymus tissue ($n=6$) was collected in sterile phosphate-buffered saline (PBS) from the surgical theater. The thymus was washed in PBS (Life Technologies) and fat and blood were dissected off. Tissue was minced into small pieces ($\sim 1\,mm^3$), followed by collagenase I (0.3 mg/mL; Sigma-Aldrich) enzymatic digestion at 37°C for 2 h. The digested tissue was poured into a 70-μm cell strainer (Falcon) and forced through the strainer using the plunger of a 10 mL syringe (BD). The strainer was continually washed with fresh medium. The resulting cell suspension was centrifuged for 5 min at 1500 rpm at 22°C. The supernatant was discarded and cells were resuspended in Dulbecco's modified Eagle medium, low glucose (DMEM; Life Technologies) with 10% HyClone fetal bovine serum (FBS; Thermo Scientific), 1% penicillin/streptomycin (P/S; Life Technologies), and basic fibroblast growth factor (FGF, 2.5 ng/μL; Peprotech) on uncoated plastic, at $\sim 1\times10^6$ cells/cm^2 density. The resulting passage (P0) cultures were kept at 37°C in a humidified

atmosphere with 5% CO_2. After 72–96 h, nonadherent cells were removed with two PBS washes. Adherent cells were cultured until confluence was reached, with feeding every 48–72 h. At this point, cells were detached using Trypsin-EDTA (0.05%; Life Technologies) and then plated at $\sim 1 \times 10^4$ cells/cm^2 in new flasks for next passage (P1).

Isolation and culture of thymus MSCs under GMP conditions

Thymus tissue was collected in sterile PBS from the surgical theater. For comparison studies, the same thymus was cut in two and GMP conditions were compared directly to standard conditions. It was then cleaned and minced in GMP quality Dulbecco's PBS (GMP PBS; Sigma-Aldrich) and enzymatically digested for a 2-h incubation with collagenase NB6 GMP (0.3 mg/mL; Serva) at 37°C. The tissue was passed through a 70-μm cell strainer, which was washed with fresh GMP PBS. Cell suspension was centrifuged at 1500 rpm at 22°C for 5 min. The supernatant was discarded and cells were resuspended in CTS StemPro MSC SFM DMEM (GMP DMEM; Life Technologies) with 10% Human Platelet Lysate (hPl; MACO Biotech) and recombinant human FGF (2.5 ng/μL; Peprotech), and were plated on uncoated plastic. The resulting passage (P0) cultures were kept at 37°C in a humidified atmosphere with 5% CO_2. After 72–96 h, nonadherent cells were removed with two washes with GMP PBS. Adherent cells were cultured in GMP DMEM, 10% hPl, and FGF with medium changes occurring every 48–72 h and then split when confluence was reached. When confluence was reached, cells were removed from plastic by washing once with GMP PBS, followed by incubation with Trypsin-EDTA (0.05%; Roche), and were then plated at $\sim 1 \times 10^4$ cells/cm^2 in new flasks for the next passage (P1).

FACS

Fluorescent-activated cell sorting analysis (FACS) was used to determine cell surface and intracellular cell marker expression. All centrifugations refer to the same conditions of 1500 rpm at 22°C for 5 min. Cells were removed from plastic with trypsin, resuspended in cold FACS Buffer (2% FBS in PBS), and centrifuged. Cells were resuspended in FACS buffer and counted. A minimum of 100,000 cells were removed for unstained control and a minimum of 200,000 cells were removed for live/dead control. Half the live/dead control cells were put on 95°C hot block for 5 min, to instigate cell death, and then cooled in the fridge. Remaining cells were stained with a viability marker (V450, Table 1) for 30 min at 4°C, then washed with cold FACS buffer and centrifuged. Supernatant was discarded and cells were resuspended such that there was 100 μL for each tube. Cell suspension was added to each tube with antibodies (Table 1) and incubated at 4°C for 30 min in the dark. During this incubation, cooled live and dead control cells were pooled and stained with the viability marker. In addition, three tubes of compensation beads (Comp Beads Plus; BD Biosciences) were stained with a fluorescein isothiocyanate (FITC), a phycoerythrin (PE), and an allophycocyanin (APC) stain, respectively.

All tubes were washed once with cold FACS buffer and centrifuged. All tubes (included unstained tube) were then incubated with cytofix/cytoperm solution (BD Pharmingen) at 4°C in the dark for 15 min. Tubes were then washed once with 1× perm/wash solution (BD Pharmingen). Tubes that did not require intracellular markers were resuspended in 300 μL FACS buffer and 100 μL 4% paraformaldehyde (PFA) (Sigma-Aldrich). Tubes with intracellular markers were resuspended in 100 μL 1× perm/wash and intracellular antibody (Table 1) and incubated in the dark at 4°C for 30 min. Tubes were then washed once in 1× perm/wash, centrifuged, and resuspended in 300 μL of FACS buffer and 100 μL 4% PFA, and stored with remaining tubes until analysis. Tubes were analyzed on a FACS Fortessa flow cytometer (BD Biosciences) using FACSDiva (BD Biosciences) for data collection and FlowJo (Treestar, Ashland) for analysis. Unstained cells, live/dead controls, and compensation beads were used to set compensation and create positive and negative gates.

In vitro *multilineage differentiation*

Multilineage differentiation into osteoblasts, adipocytes, and chondrocytes was assessed by incubating the cells, at passage between 3 and 5 (2000 cells/cm^2), in alpha MEM

Table 1. Antibodies Used for FACS Staining

Antibody	*Company*	*Color*	*Dilution*	*Catalog #*	*Measures*
CD105	R&D Systems	PE	1:20	FAB10971P	MSCs
CD90	R&D Systems	PE	1:5	FAB2067P	MSCs
CD45	R&D Systems	PE	1:20	FAB1430P	Leukocytes
CD31	BD Pharmingen	FITC	1:20	560984	Endothelial cells
CD34	eBioscience	FITC	1:40	11-0349-42	Hematopoietic stem cells
CD73	BD Pharmingen	APC	1:50	560847	MSCs
CD13	BD Pharmingen	APC	1:20	561698	MSCs
CD44	BD Pharmingen	APC	1:20	560890	MSCs
CD40	BD Pharmingen	APC	1:20	561848	Endothelial, epithelial cells
HLA-DR	BD Pharmingen	APC	1:20	560896	Human leukocytes
Fixable viability stain	BD Horizon	V450	1:1000	562247	Live/dead cells
CD166	BD Pharmingen	PE	15:100	559263	Activated leukocyte adhesion molecule
CD79alpha	BD Pharmingen	APC	1:10	551134	B cells
CD29	BD Pharmingen	APC	1:5	559883	Lymphocytes, monocytes, granulocytes
CD14	BD Pharmingen	PE	1:10	555398	Monocytes and macrophages

MSC, mesenchymal stem cell.

medium with specific StemXVivo supplement kits (R&D system) for different timescales. Osteogenic differentiation was assessed after 3 weeks of culture by Alizarin Red (Sigma-Aldrich) detection of calcific deposition. Oil Red O (Sigma-Aldrich) staining was used to detect lipidic accumulation of cells undergoing 2 weeks of adipogenic differentiation. Alcian blue (Sigma-Aldrich) staining was used to determine chondrogenic cartilage formation after 3 weeks of cell culture.

In vitro *functional studies*

All *in vitro* experiments assessing differences throughout expansion were set up with cells at P1, P3, P5, P7, P9, and P11 (P5 to P11 for senescence assay) under the same experimental settings.

For population doubling (PD) counts, cells were seeded at initial cell density of 5000 cells/cm^2 and kept in culture for 72 h. PD was calculated by using the following formula: log (end cell/start cell)/log.[2]

CFU-F (colony-forming unit-fibroblast) assay was performed by seeding cells at very low density (100 cells/cm^2) in a culture Petri dish. After 2 weeks, the dishes were stained with 3% Crystal Violet (Sigma-Aldrich) and the number of colonies was counted.

For proliferation assessment, the BrdU immunofluorescence assay (Roche) was used, according to the manufacturer's instructions.

The β-galactosidase Senescence Detection kit (Calbiochem) was used as a biomarker of senescence in MSCs. The percentage of senescent cells was represented by the number of β-galactosidase-stained cells in total population.

All *in vitro* assays were performed in triplicate wells and in six independent experiments.

Peripheral blood mononuclear cells proliferation assay

The immunosuppressive property of hT-MSCs was analyzed in coculture experiment with activated (10 μg/mL Phytoaemoagglitinin; eBioscience) allogenic peripheral blood mononuclear cells (PBMC). hT-MSCs in appropriate medium, were treated with mitomycin C (Sigma-Aldrich), 50 μg/mL for 50 min, to inactivate proliferation. Afterwards, PBMCs were freshly isolated by density-gradient centrifugation and were added to culture wells with or without hT-MSCs (MSC-PBMC, 1:10 ratio). (Co-) Cultures were maintained for 72 h, at which point BrdU labeling solution was added and cell proliferation assessed after 6 h with the fluorimetric immunoassay kit.

Multiplex analysis of cytokine production

Cytokine and growth factor production were analyzed in supernatants of PBMC alone, hT-MSCs cultured under standard and GMP conditions, and in coculture experiments (MSC–PBMC, 1:10 ratio). After 72 h of cell culture, supernatants were collected, concentrated, and analyzed using a cytokine/chemokine multiplex kit (Millipore), composed of beads for the detection of IL-2, IL-6, IL-8, INFγ, TNFα, and VEGF, according to the manufacturer's instructions. Analysis was performed using a Luminex MAGPIX instrument (Luminex Corporation).

Bioreactor

Cells were seeded on the surface of the CorMatrix scaffold at 5×10^5 cells/cm^2 and were cultured under static conditions in an appropriate medium for 1 week to allow cells to adhere. The engineered graft was then stitched to the rotating arm of a bioreactor (Harvard Apparatus) in a conduit-shape manner with the cells facing the outer side of the scaffold. The rotation was set at 0.5 rpm and slowly increased within 24 h to the final speed of 2 rpm, which was kept for 1 week. After the static and the static followed by dynamic culture, the viability of the seeded cells was assessed by a fluorescent viability/cytotoxicity assay (Life Technologies) according to the manufacturer's instruction. Seeded grafts were imaged on a Zeiss Axio Observer.Z1 with Zen Blue software (Zeiss).

Mechanical testing of the engineered graft

Nonseeded and cell-seeded CorMatrix pieces were analyzed for mechanical properties using an Instron 3343B machine (Instron, UK) with a 100 N load cell and pneumatic grips. Crosshead speed was 10 mm/min. Samples were measured for tensile stress at break using Bluehill software (Instron, UK).

In vivo *implantation of vascular grafts engineered with pig-thymus MSCs*

Three- to four-week-old female Landrace pigs of 10–15 kg were employed in this study. Animals were treated in accordance with the ''Guide for the Care and Use of Laboratory Animals'' published by the National Institutes of Health in 1996 and conforming to the ''Animals (Scientific Procedures) Act'' published in 1986. The CorMatrix was engineered with pig thymus MSCs, whose isolation, characterization, and graft engineering were performed following the same protocol used for the hT-MSCs. Surgical procedures were performed under general anesthesia and neuromuscular blockade. A left posterolateral thoracotomy was performed and a conduit-shaped graft was inserted in the left pulmonary artery. Animals were recovered with intense monitoring for the first 24 h during which period, analgesics and antibiotics were administered according to the needs.

Animals were monitored with a two-dimensional Doppler Echocardiography (VividQ; GE Healthcare) before the surgery and after 1, 2, and 3 months to assess the graft patency and blood flow. After 3 months of follow-up, pigs were euthanized and pulmonary arteries were dissected from the heart, and then fixed in 4% PFA or fresh-frozen in liquid nitrogen.

Immunohistochemistry

For paraffin embedding, samples were fixed in 4% PFA, washed in PBS, moved in to cassettes (Histosette I; Simport), processed in a Thermo Excelsior AS, and embedded in a Thermo HistoStar machine. A Sandon Finesse 325 (Thermo) microtome was used to cut 5-μm sections, which were floated onto Menzel-Glaser Superfrost Plus slides (Thermo). Slides were stored at 37°C overnight to dry completely before staining. Staining with hematoxylin and eosin (H&E) and van Gieson's (EVG) were performed using a Shandon Varistain 24-4 (Thermo). Slides were removed from machine and mounted with DPX (distyrene, a plasticizer, in toluene-xylene; Sigma-

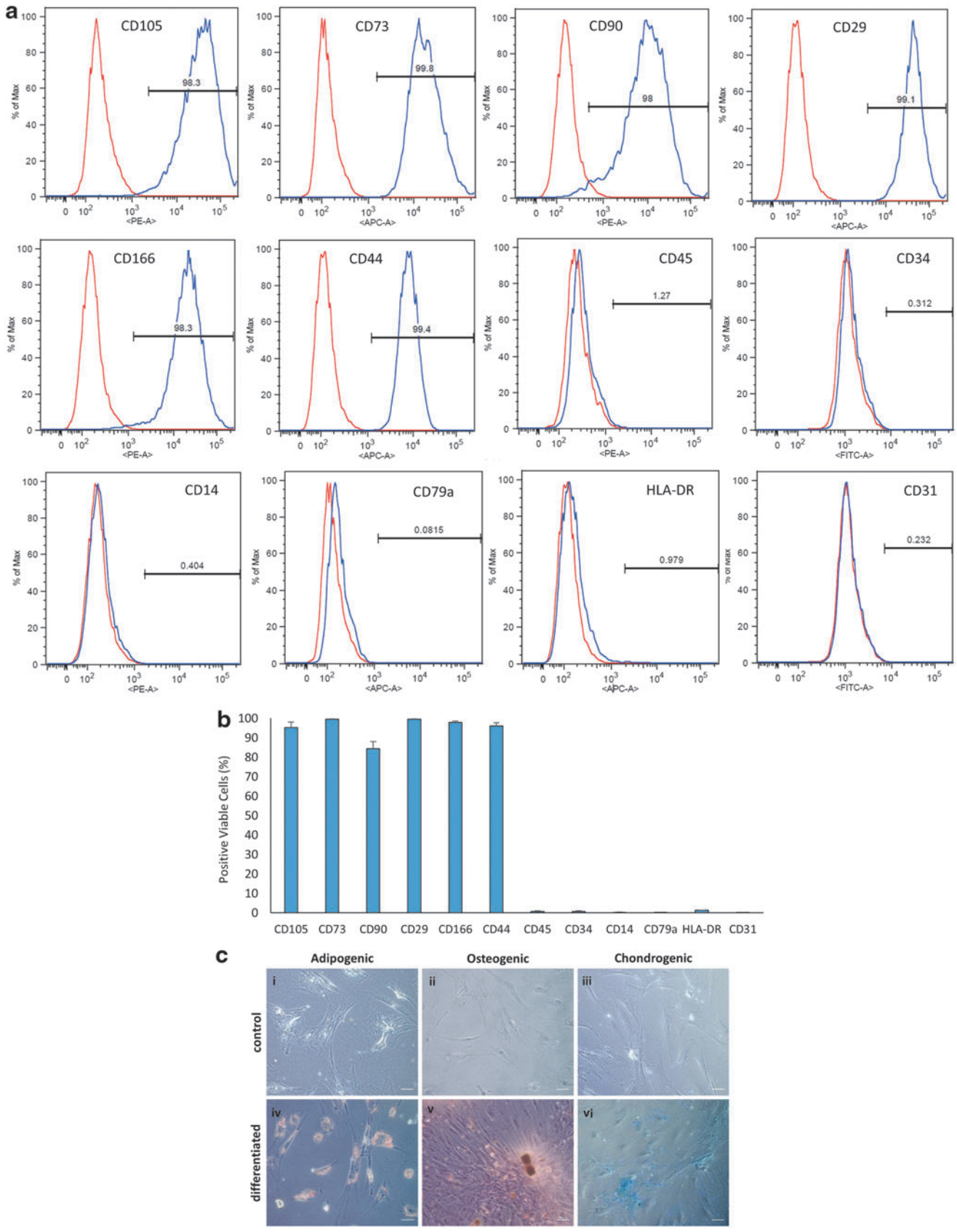

FIG. 1. Phenotypical and functional characterization of hT-MSCs at passage 2. **(a)** Representative histograms showing the expression of typical MSC markers (CD105, CD 73, CD90, CD29, CD166, and CD44) and absence of hematopoietic and endothelial markers (CD45, CD34, CD14, cd79a, HLA-DR, and CD31) by flow cytometry. **(b)** Bar graph illustrating the average of six biological replicates (mean ± SEM). **(c)** Multipotency property of hT-MSCs. Cells exhibit differentiation potential after culture in adipogenic, osteogenic, and chondrogenic media. Oil Red O was used to visualize fat droplets after adipogenic induction **(i, iv)**, Alizarin red to stain osteogenic calcium-rich deposits **(ii, v),** and Alcian blue to identify chondrogenic cartilage formation **(iii, vi)**. Results are from a single experiment representative of three independent experiments on three separate patients' hT-MSC samples. Scale bars = 50 μm. MSC, mesenchymal stem cell; SEM, standard error of the mean.

Aldrich) with 24×50 mm cover glass (VWR). Slides were imaged on a Zeiss Axio Observer.Z1 with Zen Blue software (Zeiss).

Statistical analysis

Data are expressed as mean ± SEM. Samples were analyzed by Student's *t* test or one-way analysis of variance followed by Tukey's HSD *post hoc* test. Results were considered significant if $p \leq 0.05$.

Results

Human thymus contains functional mesenchymal stem cells

After mechanical dissociation and collagenase I digestion of the pediatric patient's thymus, a cell population was obtained. Observation by microscopy at day 2 of primary culture showed that hT-MSCs adhered to the plastic surface of culture dish and presented a fibroblast-like cell morphology (Supplementary Fig. S1a, b; Supplementary Data are available online at www.liebertpub.com/tea). These cells proliferated rapidly in the expansion culture medium, acquiring a more homogeneous morphology after passage 2 (Supplementary Fig. S1c, d). At this passage (P2), flow cytometry analysis revealed that hT-MSCs exhibited the main typical MSC surface markers (CD29, CD44, CD73, CD 90, and CD 105) and were negative for hematopoietic (CD34), monocyte (CD14), leukocyte (HLA-DR, CD45), B cell (CD79alpha), and endothelial markers (CD31) (Fig. 1a, b).

To explore their functional characterization and differentiation potential, cells at early passage (P2) were induced to differentiate with osteogenic, adipogenic, or chondrogenic supplements in the culture medium. The cells showed a high degree of calcium deposition following osteogenic differentiation as confirmed by Alizarin staining. Similarly, adipogenic differentiation was estimated by positive staining of lipid vesicles using Oil Red O stain. Finally, sulfated proteoglycans, visualized by Alcian Blue staining, proved the chondrogenic differentiation of hT-MSCs (Fig. 1c).

Given that cells are often required to be passaged several times to reach an adequate number for implantation, the phenotypical and functional properties of hT-MSCs were further evaluated in later passages. The typical MSC immunophenotype and multilineage differentiation capacity were still retained at passage 5 (Supplementary Fig. S2a, b), supporting the evidence that hT-MSCs do not lose their unique properties throughout passages and can still stand as an excellent tool for stem cell therapy and/or TE cardiovascular grafts at later passages.

hT-MSCs exhibit cell attachment and growth potential onto CorMatrix scaffolds

To tissue engineer cardiovascular grafts for congenital heart disease surgery and repair, it is crucial that cells adhere and evenly proliferate onto a naturally occurring scaffold. Therefore, we tested the capability of hT-MSCs to grow and integrate into the CorMatrix®, a decellularized porcine small intestinal submucosa extracellular matrix (ECM) (Fig. 2a). Viability and cytotoxic assay showed that MSCs, grown for 2 weeks on the scaffold, were completely viable and proliferative as demonstrated by the calcein positive staining of the cells. A negligible number of dead cells was detected, as suggested by the low amount of Ethidium dye, incorporated by damaged cells (Fig. 2-i).

Histological analysis further confirms the even arrangement of the cells on the seeded scaffold (Fig. 2-ii). In addition, the EVG staining revealed that MSCs were able to synthesize their own ECM, as suggested by the positive staining for the ECM components collagens and elastin (Fig. 2-iii). An aligned, confluent cell layer could also be detected on the CorMatrix surface by scanning electron microscopy (Fig. 2-iv).

To overcome the limitations associated with traditional static culture conditions, a bioreactor was used. This system helps triggering biochemical and physical regulatory signals within seeded cells, encouraging them to grow and produce ECM to a greater extent.

The cell cultured under this dynamic system showed a greater potential for MSC growth, as detected by the calcein staining (Fig. 2-v). Furthermore, the dynamic culture allowed the cells to arrange into a tightly packed multicell layer (Fig. 2-vi, viii) and synthesize a higher amount of ECM components (Fig.-2 vii), proving that a dynamic system is essential to improve the *in vitro* development of the new tissues. This multicell layer maintained its cell phenotype as demonstrated by the expression of the MSC marker CD44 (Fig. 2c).

To determine the strength of the seeded scaffold, tensile testing was carried out. CorMatrix seeded with MSCs and

FIG. 2. Biological and mechanical characterization of the engineered grafts. hT-MSC attachment, growth, and integration into CorMatrix scaffold under standard and GMP conditions **(a, b)**. **(a)** Analysis under standard conditions. **(i, v)** Viability/Cytotoxicity Assay of hT-MSCs seeded on CorMatrix. Cells were left to grow in **(i)** static and **(v)** dynamic conditions. Calcein AM and EthD-III fluorescent probes were used to detect, respectively, live (*green* fluorescence) and dead (*red* fluorescence) cells. Scale bar = 100 μm. Histological sections and scanning electron microscopy (SEM) of hT-MSCs grown CorMatrix. H&E staining of nuclei (*black arrows*) in **(ii)** static and **(vi)** dynamic conditions. EVG staining of elastin and collagen deposition (*black arrows*) in **(iii)** static and **(vii)** dynamic conditions, respectively. Scale bar = 50 μm. SEM showing cells grown to confluence on surface of CorMatrix in **(iv)** static and **(viii)** dynamic conditions. Scale bar = 100 μm **(b)** Analysis under GMP conditions. **(ix, xiii)** Viability/Cytotoxicity Assay of GMP-cultured hT-MSCs on CorMatrix, in **(ix)** static and **(xiii)** dynamic bioreactor. Scale bar = 100 μm. **(x, xiv)** H&E and **(xi, xv)** EVG staining, and **(xii, xvi)** SEM revealed that dynamic culture system showed a greater potential for cell growth and orientation into a multicell layer. 50 μm **(x, xi, xiv, xv)**; Scale bars = 100 μm **(xii, xvi)**. **(c)** Immunostaining with the MSC marker CD44 (*green*) illustrates cells seeded on the CorMatrix (bright field) retain their mesenchymal phenotype. Scale bar = 50 μm. **(d)** Tensile strength and stiffness of the engineered graft. Ultimate tensile strength and Young's modulus were not significantly different between the CorMatrix seeded with cells and kept in dynamic conditions compared to unseeded CorMatrix. GMP, good manufacturing practices; H&E, hematoxylin and eosin; MPa, megapascal.

kept in culture for 1 week under static conditions and 1 week under dynamic conditions was compared to nonseeded CorMatrix (Control). No significant difference in the ultimate tensile strength was noted when comparing the two groups (Fig. 2d). In addition, stiffness, as measured by Young's Modulus of elasticity, was not significantly different between the two groups (Fig. 2d).

Thymus MSC-engineered graft shows in vivo *integration and regeneration of the host vascular tissue*

To assess the *in vivo* efficacy of the engineered vascular graft produced *in vitro*, we have developed a large animal model, in which the thymus MSC-engineered tissue was grafted into the piglet left pulmonary artery. Our data

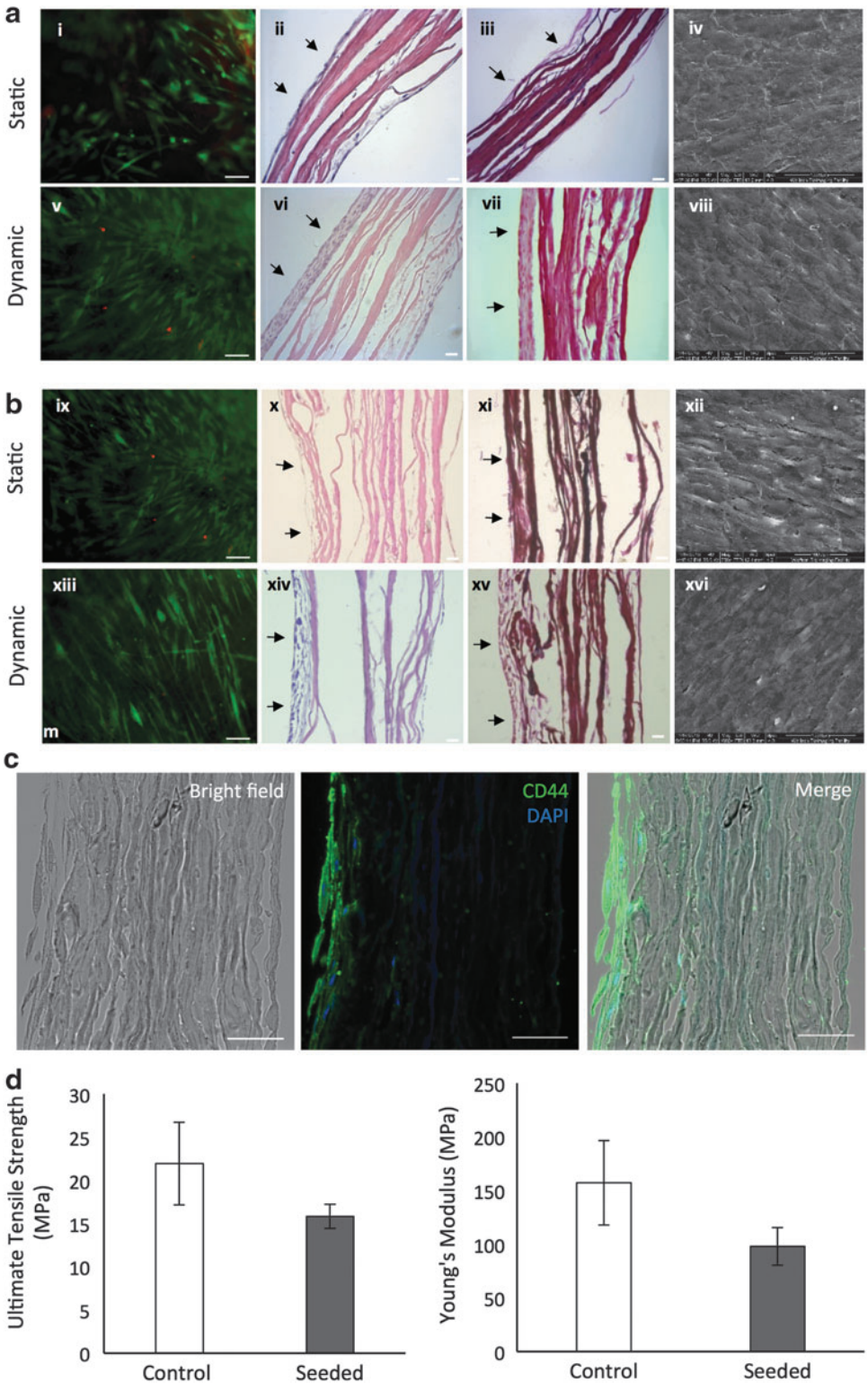

collected 3 months after *in vivo* implantation revealed that the graft was patent with no stenosis, rupture, or deformation. Macroscopic observation of the MSC-seeded graft harvested at 3 months showed smooth luminal surfaces without signs of thrombosis and tissue degradation (Fig. 3a, b). Histological analysis of the explanted tissue showed that the graft exhibited an extensive nucleation throughout its structure (Fig. 3c, d).

In addition, the immunohistochemical analysis showed an organized multilayer of smooth muscle cells populating the tunica media (Fig. 3e, f). Furthermore, immunohistochemical and electron scanning microscopy showed a newly formed layer of endothelial cells in the luminal side of the graft (Fig. 3e, f, h, i). Finally, the observation of new vessels in the adventitia provides a good indication of neovascularization, which is important for oxygenation and nutrient supply within the graft (Fig. 3g).

hT-MSCs retain phenotype and differentiation properties after culture under GMP conditions

After proving that the human thymus, surgically removed during neonatal cardiac repair, can be an excellent source of MSCs, we next optimized a xeno-free culture system, compliant with GMP standard.

Phenotypic analysis of hT-MSCs cultured under GMP-compliant conditions revealed that cells retained the typical MSC markers throughout passages (P2–P5) and absence of immune, hematopoietic, and endothelial markers (Fig. 4a and Supplementary Fig. S3a). In addition, the differentiation

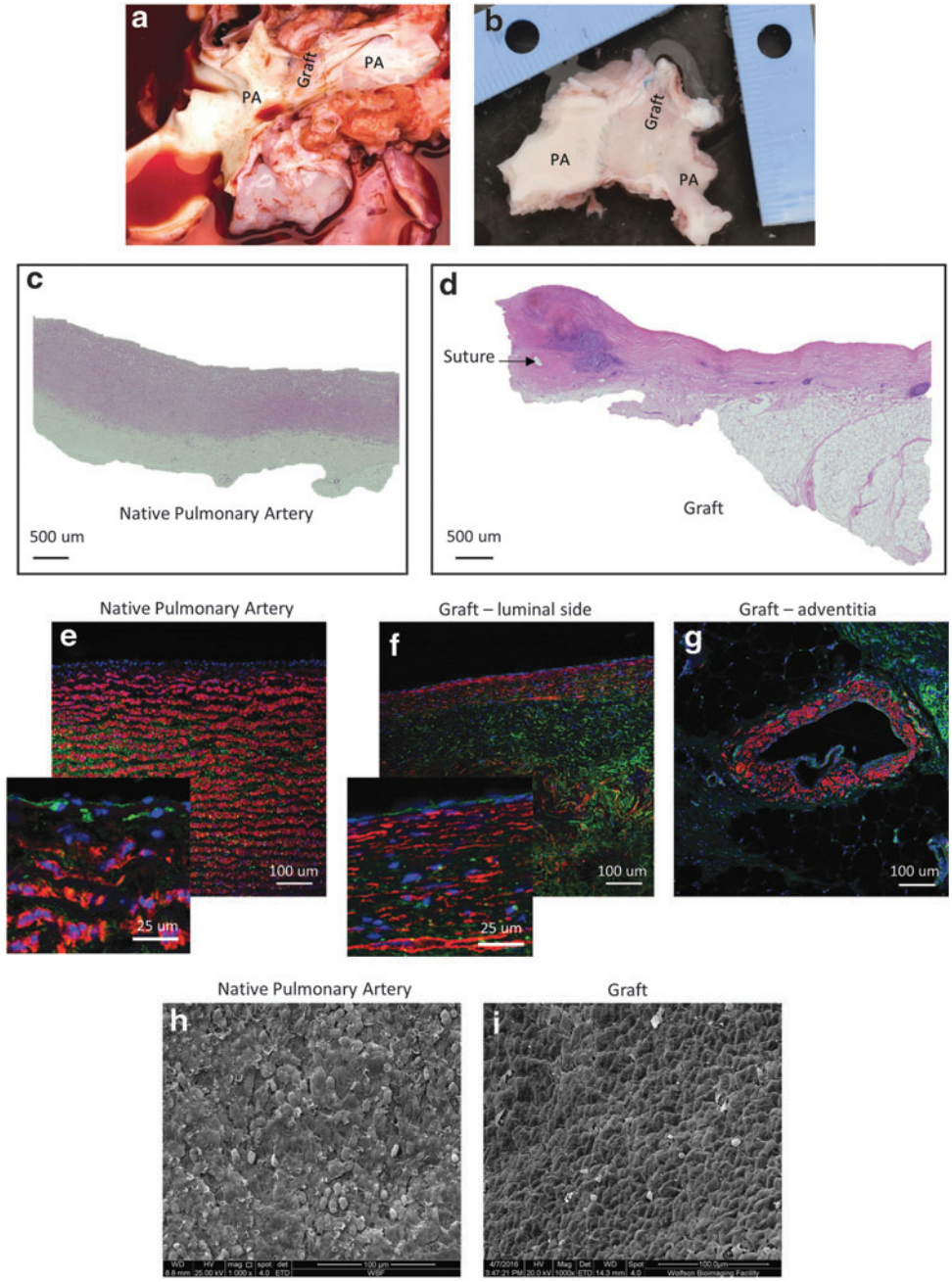

FIG. 3. *In vivo* explantation of CorMatrix seeded with thymus MSCs. **(a, b)** Macroscopic images showing the cut-open left pulmonary artery. The graft has similar macroscopic morphology to surrounding native pulmonary artery (PA) tissue. **(c, d)** H&E staining of the native pulmonary artery compared to explanted graft. The graft H&E has extensive nucleation. **(e–g)** Immunohistochemistry of the native pulmonary artery compared to explanted graft. Smooth muscle actin (*red*) staining and isolectin staining (*green*) illustrate a multi-smooth muscle cell layer and a luminal endothelial cell layer in native tissue **(e)** and graft **(f)**. **(g)** The adventitia shows vascularization. Scanning electron micrographs of the luminal surface shows the topography of endothelial cell layer in the native tissue **(h)** and the graft **(i)**.

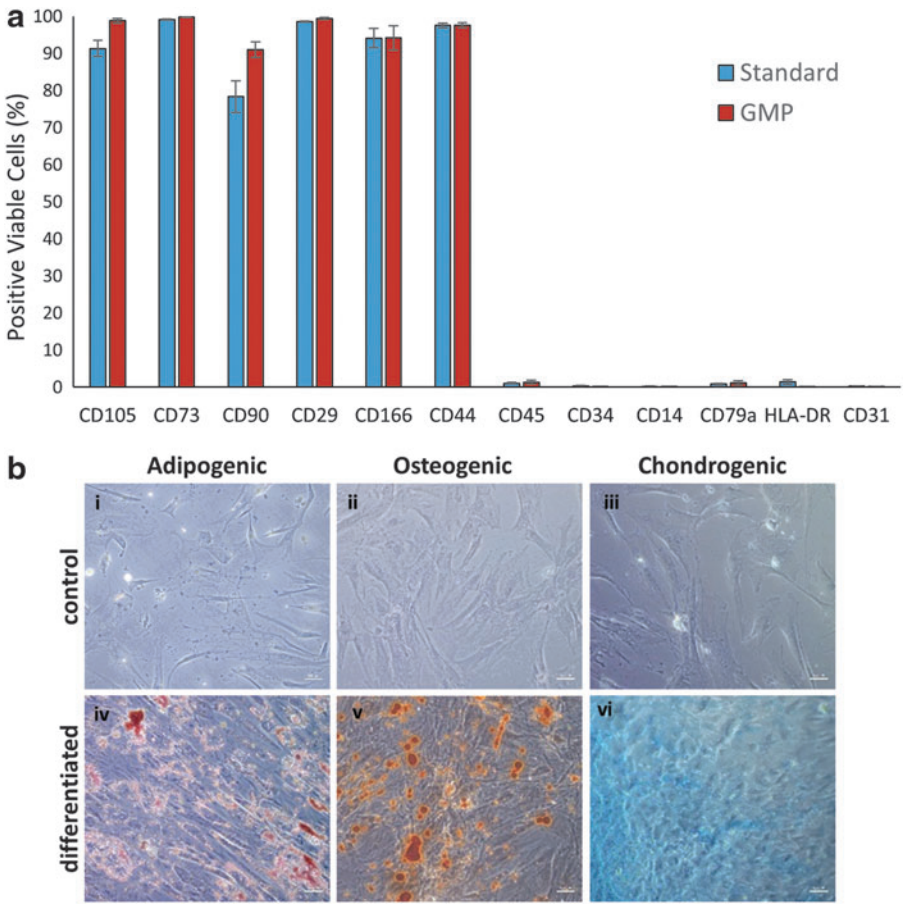

FIG. 4. Phenotypical and functional analysis of hT-MSCs cultured under standard (non-GMP) and GMP-compliant conditions. **(a)** FACS analysis reveals comparable expression of typical MSC markers and absence of hematopoietic and endothelial markers in hT-MSCs cultured under standard and GMP conditions at passage 5. **(b)** Multipotency evaluation of hT-MSCs cultured under GMP-compliant conditions at passage 5. hT-MSCs retain differentiation potential after culture in **(i, iv)** adipogenic (Oil Red O staining), **(ii, v)** osteogenic (Alizarin staining), and **(iii, vi)** chondrogenic (Alcian Blue) inducing media. Scale bars = 50 μm.

capacity was conserved, after culture in adipogenic-, osteogenic-, and chondrogenic-supplemented media both at earlier and later passages (Fig. 4b and Supplementary Fig. S3b).

hT-MSCs cultured under GMP conditions exhibit better functional behavior compared to standard cultured conditions

Functional features were next assessed to determine whether the GMP-optimized culture conditions affected cell growth and viability. Therefore, a battery of *in vitro* assays was performed to address differences in growth potential, by analyzing proliferation and senescence throughout the expansion.

BrdU incorporation revealed a significantly higher level of proliferation activity when MSCs were cultured under GMP media (observed at P5). For both culture conditions, a trend toward decreased proliferation was seen at later passages, although not statistically significant (Fig. 5a).

The clonogenic capacity and growth kinetics were also evaluated. The CFU assay and PD were, respectively, comparable between the standard and GMP condition at early passages (Fig. 5b, c). It may be worth noting that GMP-cultured cells exhibited a trend toward higher number of colony and more PD at higher passages, although not statistically significant. The incidence of cell senescence was lower in GMP-cultured MSCs, as suggested by the lower activity of the β-galactoside enzyme (Fig. 5d, e). Taken together, these data prove that hT-MSC behavior is not affected, but rather improved, by the change of culture condition, from standard to a GMP-optimized system.

hT-MSCs cultured under standard and GMP conditions display comparable levels of protein secretion and immunosuppressive capacity

Proteins secretion was also compared by analyzing the secretome of hT-MSCs cultured under standard and GMP conditions. Inflammatory cytokines, such as IFNγ, IL-2, and TNFα, were expressed at very low levels in both media, while the immunomodulatory IL-6 and the angiogenic factor VEGF were secreted in higher amount. However, no significant differences were detected between the two media. Interestingly, only the chemokine IL-8 was found to be significantly higher in the secretome of GMP-cultured hT-MSCs (Fig. 6a).

Immunosuppressive capacity of the cells cultured in both conditions was tested by evaluating the ability to suppress allogenic PBMC proliferation. When cocultured with hT-MSCs, activated PBMC significantly reduced their proliferation rate (Fig. 6b). In addition, the secretion of immunomodulatory cytokine by PBMC was also significantly decreased with cocultured hT-MSCs under both standard and GMP conditions, further demonstrating that hT-MSC-immunosuppressive capacity was maintained when cultured under both standard and GMP conditions (Fig. 6c).

hT-MSCs growth potential on CorMatrix is retained under static and dynamic GMP culture conditions

Finally, the growth potential of MSCs cultured on the CorMatrix scaffold, in GMP conditions was assessed

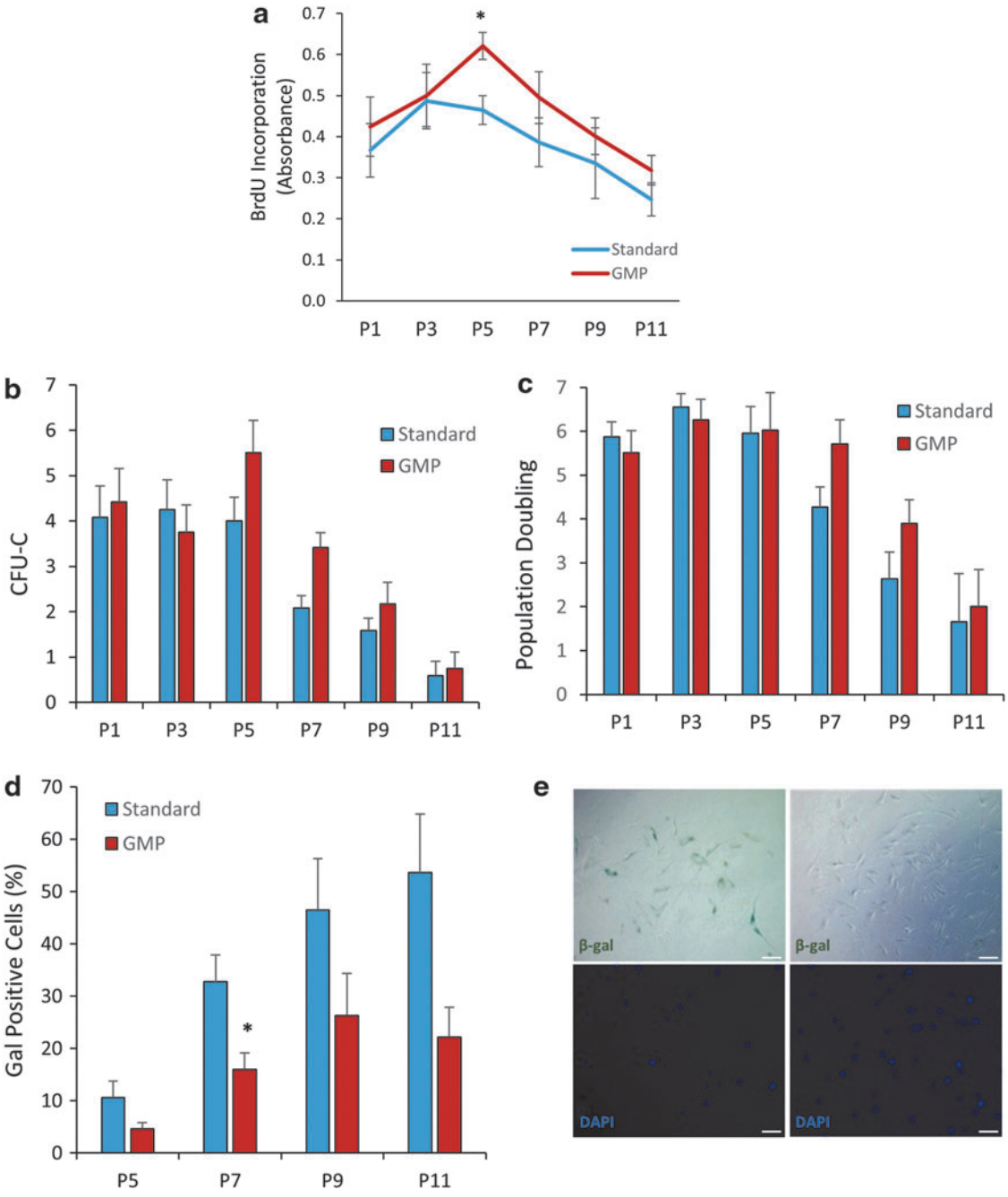

FIG. 5. *In vitro* functional assessments during hT-MSC expansion. **(a–c)** Growth potential analyzed by **(a)** BrdU incorporation, **(b)** colony-forming unit, and **(c)** population doubling revealed a comparable or even better performance of hT-MSCs cultured under GMP conditions, compared to standard, non-GMP, conditions. **(d, e)** Incidence of senescence, measured by **(d)** β-galactosidase activity, was lower in GMP-cultured MSCs. **(e)** Representative images of β-galactosidase-positive cells (*green* stain). Scale bar = 100 μm; nuclei counter stain (DAPI) was used for cell count normalization. Data are expressed as mean—SEM of six experiments. $*p < 0.05$ versus control.

(Fig. 2b). Viability/cytotoxicity assay and histological analysis of the seeded scaffolds were carried out under this growth condition. A large amount of viable cells, detected by calcein incorporation, was observed when cells were cultured under the static and, to a higher extent, under the dynamic system provided in the bioreactor (Fig. 2-ix, xiii). As seen for the MSCs grown under a standard culture condition (Fig. 2a), the bioreactor proved to be a crucial factor in helping the cell growth and synthesis of ECM, as the H&E staining of nuclei and EVG staining of collagen and elastin showed (Fig. 2-x, xiv, xi, xv).

Furthermore, images from scanning electron microscopy showed a greater potential for cell growth and orientation into a multicell layer under a dynamic culture system compared to static conditions (Fig. 2-xii, xvi). This finding represents an important step toward the clinical-grade

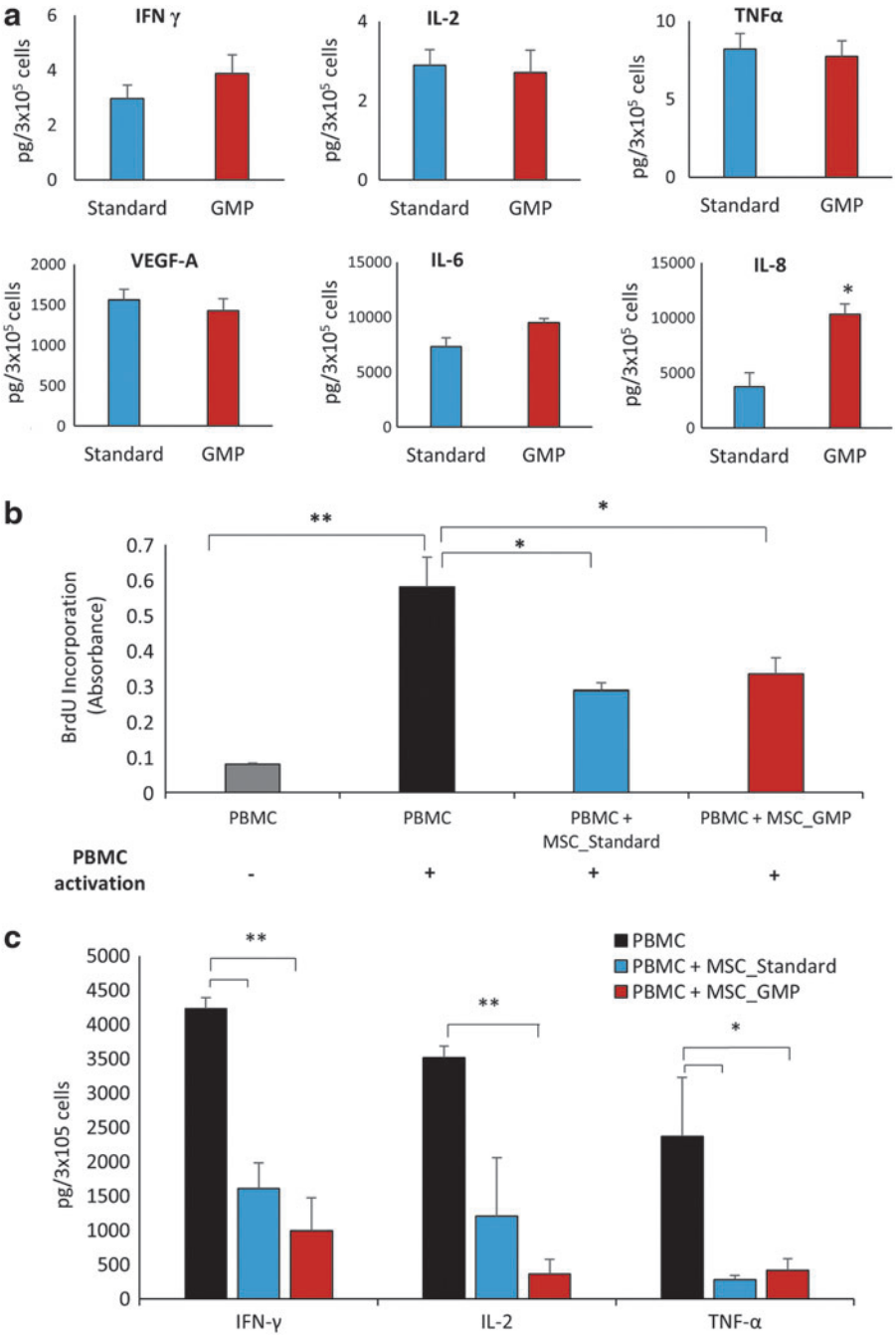

FIG. 6. Analysis of protein secretion and immunosuppressive capacity of hT-MSCs. **(a)** Graphs showing the quantification of cytokines, growth factors, and chemokines (pg/3×10^5 cells) released by hT-MSCs cultured under standard and GMP conditions. **(b)** BrdU incorporation assay showing a reduction of the proliferation of activated PBMC in coculture with MSCs under standard and GMP conditions. **(c)** Quantification of immunomodulatory factors released by PBMC alone and in coculture with hT-MSCs. Upon coculture of MSCs with activated PBMC, lower amount of immunomodulatory proteins could be detected in PBMC supernatants, compared to PBMC culture alone. Data are expressed as mean—SEM of four or five experiments ($*p < 0.05$; $**p < 0.005$). PBMC, peripheral blood mononuclear cell.

realization of an engineered cardiovascular graft using MSCs derived from human thymus tissues.

Discussion

MSCs have gained significant attention in the last decades. The easy accessibility and versatile biological properties, due to their high proliferative capacity and multilineage differentiation potential, have suggested that MSCs may represent a useful therapeutic tool for various disorders.[36] To the best of our knowledge, this report represents the first study of a systematic and extensive culture of MSCs derived from human thymus and their use in the production of tissue-engineered grafts for CHD repair.

Although previously suggested as a potential source of MSCs, the thymus has little been regarded as a potential tool for regenerative medicine, due to the invasive procedure of its removal. However, a thymectomy is often necessary for surgical access in the correction of many CHD, the most common birth defect worldwide.[23] Hence, this normally discarded tissue can become a precious source of autologous stem cells to be used in the correction of the child's defect.

The thymus-derived MSCs we have isolated, homogeneously expressed the typical marker and multilineage differentiation capacity of MSCs throughout passages. This is crucial, given that MSCs to be used for CHD require an intensive cell culture and propagation. In fact, unlike other cardiovascular repair, such as myocardial infarction or

cardiomyopathy where the use of MSCs have been extensively investigated,[13,37] in CHD, some anatomic structures of the heart are usually absent or highly compromised and MSCs cannot simply be injected to the defective site. Therefore, a surgical correction to introduce or replace the compromised structure is the only treatment.

The current cardiovascular grafts used for corrective heart surgery did not prove to be effective for the long-term repair, due to limited durability and patency and recurrent calcification episodes.[28,38,39] TE, by combining autologous MSCs and biocompatible scaffolds, potentially offers the solution to this limitation. The production of tissue-engineered constructs requires an extensive cell culture process and an optimal environment for the growth of the graft. Our thymus-derived MSCs showed a high proliferation rate during expansion, which was retained when cells were cultured onto different biological scaffolds (unpublished data).

For the potential clinical translation of this work, we have focused on the commercially available CorMatrix, a decellularized porcine small intestinal submucosa, currently in use in cardiac reconstruction procedures. Unlike other materials used in cardiac defect corrective surgery, the CorMatrix holds the advantage of avoiding the immune response associated with xenograft and homograft materials.[40–42] In addition, as a decellularized biological scaffold, it possesses the potential for the accommodation and growth of host cells, which is an essential feature in TE. For this reason, and for being a scaffold already approved by the Federal Drug Administration (FDA) for use in cardiovascular repair, we have chosen the CorMatix as the most suitable scaffold for the realization of the MSC-engineered graft and the potential clinical translation of this work.

Clinical data about CorMatrix used in routine congenital heart surgical repair have shown, so far, favorable outcomes; however, long-term follow-up are missing.[43,44] Woo *et al.* have histologically examined CorMatrix materials explanted from pediatric patients undergoing open heart surgeries. Despite an overall favorable clinical outcome for patients, the explanted specimens showed a high degree of fibrosis and chronic inflammation, with no patch recellularization or integration within the surrounding tissue.[45] The *in vitro* repopulation of decellularized patches has proved to provide a significantly higher integration, regeneration, and function of the tissue when implanted in animal models.[46,47] Investigations are currently being conducted to identify the ideal human cell types for use in cardiovascular TE.

The finding that our isolated and characterized hT-MSCs can sustain growth and proliferation on the CorMatrix makes them a favorable candidate for TE cardiovascular grafts for CHD. In addition, our study provides an *in vivo* proof of concept that our engineered graft can be safely used in a left pulmonary artery position.

For this animal-based preclinical study, we have used a porcine model, whose cardiovascular system more closely resembles the anatomy and function of a human counterpart.[48] In addition, such large animal model has the advantage of a longer life span and a rapid growth speed, which facilitate longitudinal studies critical for stem cells and TE applications. Besides proving the safety of our engineered graft, the piglet model allowed us to optimize the size and shape of the scaffold and develop a surgical procedure suitable for clinical application.

The surgical technique developed by our group, which consists of the reconstruction of the left pulmonary artery, can serve as a suitable model for some complex CHD such as pulmonary atresia or truncus arteriosus, where the pulmonary artery has to be reconnected to the right ventricle with a conduit. Our study demonstrates the capacity of the hT-MSC tissue-engineered conduit to effectively engraft in the host pulmonary artery. Furthermore, 3 months after implantation, the MSC-engineered graft exhibited a good integration within the host-surrounding site, with no evidence of thrombosis, occlusion, or stenosis.

In addition to the structural support to the graft, the presence of MSCs on the scaffold can be beneficial in providing the microenvironment for local tissue regeneration. It has become clear that MSCs exhibit both a trophic and immunomodulatory activity, which drive the vascular cell recruitment and the reduction of immune response, respectively.[8] By conducting a multiplex analysis of cytokine and chemokine production, we found that hT-MSCs release a high amount of VEGF, IL-6, and IL-8, compared to other factors. VEGF is a recognized chemotactic factor for endothelial cells.[49,50] In addition, it has been demonstrated that it can exert an indirect immunosuppressive effect by increasing the secretion of indoleamine 2,3-dioxygenase, a negative regulator of immune response, by dendritic cells, thus affecting lymphocyte proliferation and activation.[51] IL-8 has also been shown to exhibit proangiogenic effect by promoting endothelial cell proliferation and migration.[52]

In this study, electron microscopy and immunocytochemistry analysis of the explanted graft indicated the building of a layer of endothelial cells on the luminal side of the graft. Furthermore, a consistent amount of cell growth is also evident in the tunica media and the adventitia, where vessel-like structures could be observed, providing the evidence of a neovascularization occurring in the graft. However, a longer term follow-up may be needed to observe a complete cell repopulation identical to the structure of the native pulmonary artery.

Among the soluble factors released in the conditioned medium, a great amount of IL-6 was also detected. Despite its well-established role as an immune-suppressive factor, recent evidences have pointed to IL-6 as an anti-inflammatory cytokine. These studies showed that IL-6 can suppress the secretion of many proinflammatory cytokines and exerts anti-inflammatory effect both locally and systemically.[53,54] In addition, it has been shown that, when IL-6 is downregulated in MSCs, cells lose their immune privilege by changing the expression pattern of MHC surface antigens and triggering cell rejection after implantation.[55] The abundant secretion of these immunomodulatory factors by hT-MSCs might be responsible for the reduction of blood mononuclear cell proliferation and proinflammatory cytokine secretion that we observed in cocultures of the two cell types.

As for all MSCs with a potential use in cell-based therapies, the establishment of a manufacturing process that ensures the highest quality and safety of an hT-MSC-derived engineered vascular graft is an important prerequisite for clinical applications. The safest option to obtain a clinical-grade tissue-engineered vascular graft using hT-MSCs would be to perform the whole manufacturing process, from cell isolation through the production of the graft, in GMP-compatible conditions.[34] To attain GMP standards,

one main requirement is to use animal-free products during *in vitro* culture establishment and expansion of the cells, to avoid the risk of graft rejection, immunoreactions, and infections in the patient.[32,33]

In this study, we have established GMP-compliant culture conditions for hT-MSCs and performed a systematic comparison between hT-MSCs isolated and cultured under a standard procedure, which involves the use of xenogenic supplements, and GMP conditions, using xeno-free reagents. GMP-grade recombinant enzymes and growth factors were used to replace animal-derived equivalents, while human platelet lysate proved to be a good GMP-compliant alternative to FBS.

Results from our work show that hT-MSCs cultured in our optimized GMP-compliant xeno-free medium retained the phenotypical, multipotency and immunogenicity properties observed with standard cell culture. In addition, the hT-MSC high proliferative capacity is not lost, but rather increased, when cells are cultured under xeno-free conditions. This is an important finding, given that an extensive *ex vivo* expansion is required to reach an adequate cell number for the production of the engineered graft. Furthermore, after extensive culture expansion, senescence becomes critical. In this study, we demonstrated that hT-MSCs cultured in the GMP-compliant system undergo senescence more slowly than cells cultured under standard condition.

Most importantly, the ability of hT-MSCs to grow and engraft on the CorMatrix was retained in the xeno-free system. In addition, the growth potential of hT-MSCs in both conditions was further increased when cells were cultured in a dynamic culture system provided by a bioreactor. In fact, static culture can impair diffusion of nutrients and O_2 through the scaffold; therefore, it is important that the graft is grown in a system that closely resembles the physiological environment. The bioreactor mimics *in vitro* the physical effect of blood flow and ensures that nutrients and O_2 are homogeneously diffused to the three-dimensional tissue constructs, overcoming the limit of static cultures.

Collectively, our findings show for the first time that hT-MSCs are a suitable candidate for the production of a tissue-engineered cardiovascular graft. Furthermore, the optimization of a xeno-free, GMP-compliant culture proved to be an optimum system for the large-scale expansion of hT-MSCs and the production of a tissue-engineered cardiovascular graft, without compromising the quality of the cells. This study represents an important step in preparing and scaling up hT-MSC production for potential therapeutic use in children with CHD. It demonstrated the feasibility of engineering clinical-grade living autologous replacement graft using thymus MSCs and proved the biocompatibility and efficacy of such a graft for *in vivo* implantation and integration.

Longer-term preclinical studies are needed to confirm the efficacy and safety of the engineered graft. Given the rapid porcine growth rate, 6 months to 1 year of follow-up will enable to determine whether the implanted graft will keep its patency and function into an adult size pig, which closely reflects the human growth. Once the long-term effectiveness and biosafety of the bioengineered graft will be proved, the transition from bench to bedside will require the establishment of a quality control approach to ensure that the manufacturing process (from the facilities, through the equipment, raw materials, and personnel qualification) meets the relevant local and national regulatory requirements.[56] The establishment of a GMP-compliant protocol for an hT-MSC-derived vascular graft by our group ensures that the engineered tissue is produced in a reproducible manner and meets the required specification to deliver an absolutely safe and effective tissue-engineered product for cardiac congenital defect repair.

Acknowledgments

We are grateful to Dr. Andrew Parry and Dr. Serban Stoica for helping with thymus collection, and to Dr. Nandita Singh for her technical assistance. We also wish to acknowledge the assistance of Dr. Andrew Herman and Lorena Sueiro Ballesteros from the University of Bristol Faculty of Biomedical Sciences Flow Cytometry Facility. This study was supported by the Sir Jules Thorn Charitable Trust, the Enid Linder Foundation, and NIHR Bristol Biomedical Research Unit in Cardiovascular Medicine.

Author Contributions

M.T.G. and M.C. conceived and designed the research. D.I., M.M.S., and A.A. performed experiments. M.M.S. and D.I. analyzed data. M.M.S., D.I., and M.T.G. interpreted results of experiments. D.I. and M.M.S. prepared figures. D.I., M.M.S., and M.T.G. drafted and edited the article. M.T.G. and M.C. revised the article. All authors read and approved the final article.

Disclosure Statement

No competing financial interests exist.

References

1. Young, H.E., and Black, A.C., Jr. Adult stem cells. Anat Rec A Discov Mol Cell Evol Biol **276,** 75, 2004.
2. Pittenger, M.F., Mackay, A.M., Beck, S.C., *et al.* Multilineage potential of adult human mesenchymal stem cells. Science **284,** 143, 1999.
3. Dominici, M., Le Blanc, K., Mueller, I., *et al.* Minimal criteria for defining multipotent mesenchymal stromal cells. The International Society for Cellular Therapy position statement. Cytotherapy **8,** 315, 2006.
4. Crisan, M., Yap, S., Casteilla, L., *et al.* A perivascular origin for mesenchymal stem cells in multiple human organs. Cell Stem Cell **3,** 301, 2008.
5. da Silva Meirelles, L., Caplan, A.I., and Nardi, N.B. In search of the in vivo identity of mesenchymal stem cells. Stem Cells **26,** 2287, 2008.
6. Caplan, A.I. All MSCs are pericytes? Cell Stem Cell **3,** 229, 2008.
7. Guimaraes-Camboa, N., Cattaneo, P., Sun, Y., *et al.* Pericytes of multiple organs do not behave as mesenchymal stem cells in vivo. Cell Stem Cell **20,** 345, 2017.
8. Caplan, A.I., and Hariri, R. Body management: mesenchymal stem cells control the internal regenerator. Stem Cells Transl Med **4,** 695, 2015.
9. Horwitz, E.M., Prockop, D.J., Fitzpatrick, L.A., *et al.* Transplantability and therapeutic effects of bone marrow-derived mesenchymal cells in children with osteogenesis imperfecta. Nat Med **5,** 309, 1999.

10. Horwitz, E.M., Prockop, D.J., Gordon, P.L., *et al.* Clinical responses to bone marrow transplantation in children with severe osteogenesis imperfecta. Blood **97,** 1227, 2001.
11. Horwitz, E.M., Gordon, P.L., Koo, W.K., *et al.* Isolated allogeneic bone marrow-derived mesenchymal cells engraft and stimulate growth in children with osteogenesis imperfecta: implications for cell therapy of bone. Proc Natl Acad Sci U S A **99,** 8932, 2002.
12. Baron, F., Lechanteur, C., Willems, E., *et al.* Cotransplantation of mesenchymal stem cells might prevent death from graft-versus-host disease (GVHD) without abrogating graft-versus-tumor effects after HLA-mismatched allogeneic transplantation following nonmyeloablative conditioning. Biol Blood Marrow Transplant **16,** 838, 2010.
13. Chen, S.L., Fang, W.W., Ye, F., *et al.* Effect on left ventricular function of intracoronary transplantation of autologous bone marrow mesenchymal stem cell in patients with acute myocardial infarction. Am J Cardiol **94,** 92, 2004.
14. Jiang, S., Haider, H., Idris, N.M., Salim, A., and Ashraf, M. Supportive interaction between cell survival signaling and angiocompetent factors enhances donor cell survival and promotes angiomyogenesis for cardiac repair. Circ Res **99,** 776, 2006.
15. Zhang, S., Ge, J., Sun, A., *et al.* Comparison of various kinds of bone marrow stem cells for the repair of infarcted myocardium: single clonally purified non-hematopoietic mesenchymal stem cells serve as a superior source. J Cell Biochem **99,** 1132, 2006.
16. Kharaziha, P., Hellstrom, P.M., Noorinayer, B., *et al.* Improvement of liver function in liver cirrhosis patients after autologous mesenchymal stem cell injection: a phase I-II clinical trial. Eur J Gastroenterol Hepatol **21,** 1199, 2009.
17. Mohamadnejad, M., Namiri, M., Bagheri, M., *et al.* Phase 1 human trial of autologous bone marrow-hematopoietic stem cell transplantation in patients with decompensated cirrhosis. World J Gastroenterol **13,** 3359, 2007.
18. Ngoc, P.K., Phuc, P.V., Nhung, T.H., Thuy, D.T., and Nguyet, N.T. Improving the efficacy of type 1 diabetes therapy by transplantation of immunoisolated insulin-producing cells. Hum Cell **24,** 86, 2011.
19. Mouiseddine, M., Mathieu, N., Stefani, J., Demarquay, C., and Bertho, J.M. Characterization and histological localization of multipotent mesenchymal stromal cells in the human postnatal thymus. Stem Cells Dev **17,** 1165, 2008.
20. Janeway, C., Murphy, K., Travers, P., and Walport, M. Immunobiology. Janeway's immunobiology. 7th ed. New York: Garland Science, 2008.
21. Steinmann, G.G. Changes in the human thymus during aging. Curr Top Pathol **75,** 43, 1986.
22. von Gaudecker, B. The development of the human thymus microenvironment. Curr Top Pathol **75,** 1, 1986.
23. Roosen, J., Oosterlinck, W., and Meyns, B. Routine thymectomy in congenital cardiac surgery changes adaptive immunity without clinical relevance. Interact Cardiovasc Thorac Surg **20,** 101, 2015.
24. Rzhaninova, A.A., Gornostaeva, S.N., and Goldshtein, D.V. Isolation and phenotypical characterization of mesenchymal stem cells from human fetal thymus. Bull Exp Biol Med **139,** 134, 2005.
25. Krampera, M., Marconi, S., Pasini, A., *et al.* Induction of neural-like differentiation in human mesenchymal stem cells derived from bone marrow, fat, spleen and thymus. Bone **40,** 382, 2007.
26. Siepe, M., Thomsen, A.R., Duerkopp, N., *et al.* Human neonatal thymus-derived mesenchymal stromal cells: characterization, differentiation, and immunomodulatory properties. Tissue Eng Part A **15,** 1787, 2009.
27. Krampera, M., Sartoris, S., Liotta, F., *et al.* Immune regulation by mesenchymal stem cells derived from adult spleen and thymus. Stem Cells Dev **16,** 797, 2007.
28. Allen, B.S., El-Zein, C., Cuneo, B., Cava, J.P., Barth, M.J., and Ilbawi, M.N. Pericardial tissue valves and Gore-Tex conduits as an alternative for right ventricular outflow tract replacement in children. Ann Thorac Surg **74,** 771, 2002.
29. Lange, R., Weipert, J., Homann, M., *et al.* Performance of allografts and xenografts for right ventricular outflow tract reconstruction. Ann Thorac Surg **71,** S365, 2001.
30. Alghamdi, M.H., Mertens, L., Lee, W., Yoo, S.J., and Grosse-Wortmann, L. Longitudinal right ventricular function is a better predictor of right ventricular contribution to exercise performance than global or outflow tract ejection fraction in tetralogy of Fallot: a combined echocardiography and magnetic resonance study. Eur Heart J Cardiovasc Imaging **14,** 235, 2013.
31. Cheung, M.M., Konstantinov, I.E., and Redington, A.N. Late complications of repair of tetralogy of Fallot and indications for pulmonary valve replacement. Semin Thorac Cardiovasc Surg **17,** 155, 2005.
32. Tonti, G.A., and Mannello, F. From bone marrow to therapeutic applications: different behaviour and genetic/epigenetic stability during mesenchymal stem cell expansion in autologous and foetal bovine sera? Int J Dev Biol **52,** 1023, 2008.
33. van der Valk, J., Brunner, D., De Smet, K., *et al.* Optimization of chemically defined cell culture media—replacing fetal bovine serum in mammalian in vitro methods. Toxicol In Vitro **24,** 1053, 2010.
34. Bieback, K., Kinzebach, S., and Karagianni, M. Translating research into clinical scale manufacturing of mesenchymal stromal cells. Stem Cells Int **2010,** 193519, 2011.
35. Sensebe, L., and Bourin, P. Mesenchymal stem cells for therapeutic purposes. Transplantation **87,** S49, 2009.
36. Deans, R.J., and Moseley, A.B. Mesenchymal stem cells: biology and potential clinical uses. Exp Hematol **28,** 875, 2000.
37. Chen, S., Liu, Z., Tian, N., *et al.* Intracoronary transplantation of autologous bone marrow mesenchymal stem cells for ischemic cardiomyopathy due to isolated chronic occluded left anterior descending artery. J Invasive Cardiol **18,** 552, 2006.
38. Tweddell, J.S., Pelech, A.N., Frommelt, P.C., *et al.* Factors affecting longevity of homograft valves used in right ventricular outflow tract reconstruction for congenital heart disease. Circulation **102,** III130, 2000.
39. Vaideeswar, P., Mishra, P., and Nimbalkar, M. Infective endocarditis of the Dacron patch-a report of 13 cases at autopsy. Cardiovasc Pathol **20,** e169, 2011.
40. Rajani, B., Mee, R.B., and Ratliff, N.B. Evidence for rejection of homograft cardiac valves in infants. J Thorac Cardiovasc Surg **115,** 111, 1998.
41. Gock, H., Murray-Segal, L., Salvaris, E., Cowan, P., and D'Apice, A.J. Allogeneic sensitization is more effective than xenogeneic sensitization in eliciting Gal-mediated skin graft rejection. Transplantation **77,** 751, 2004.
42. Ross, J.R., Kirk, A.D., Ibrahim, S.E., Howell, D.N., Baldwin, W.M., 3rd, and Sanfilippo, F.P. Characterization of human anti-porcine ''natural antibodies'' recovered from ex vivo perfused hearts—predominance of IgM and IgG2. Transplantation **55,** 1144, 1993.

43. Quarti, A., Nardone, S., Colaneri, M., Santoro, G., and Pozzi, M. Preliminary experience in the use of an extracellular matrix to repair congenital heart diseases. Interact Cardiovasc Thorac Surg **13,** 569, 2011.
44. Scholl, F.G., Boucek, M.M., Chan, K.C., Valdes-Cruz, L., and Perryman, R. Preliminary experience with cardiac reconstruction using decellularized porcine extracellular matrix scaffold: human applications in congenital heart disease. World J Pediatr Congenit Heart Surg **1,** 132, 2010.
45. Woo, J.S., Fishbein, M.C., and Reemtsen, B. Histologic examination of decellularized porcine intestinal submucosa extracellular matrix (CorMatrix) in pediatric congenital heart surgery. Cardiovasc Pathol **25,** 12, 2016.
46. Robertson, M.J., Dries-Devlin, J.L., Kren, S.M., Burchfield, J.S., and Taylor, D.A. Optimizing recellularization of whole decellularized heart extracellular matrix. PLoS One **9,** e90406, 2014.
47. Zhao, Y., Zhang, S., Zhou, J., *et al.* The development of a tissue-engineered artery using decellularized scaffold and autologous ovine mesenchymal stem cells. Biomaterials **31,** 296, 2010.
48. Suzuki, Y., Yeung, A.C., and Ikeno, F. The representative porcine model for human cardiovascular disease. J Biomed Biotechnol **2011,** 195483, 2011.
49. Lamalice, L., Le Boeuf, F., and Huot, J. Endothelial cell migration during angiogenesis. Circ Res **100,** 782, 2007.
50. Wang, Y., Zang, Q.S., Liu, Z., *et al.* Regulation of VEGF-induced endothelial cell migration by mitochondrial reactive oxygen species. Am J Physiol Cell Physiol **301,** C695, 2011.
51. Marti, L.C., Pavon, L., Severino, P., Sibov, T., Guilhen, D., and Moreira-Filho, C.A. Vascular endothelial growth factor-A enhances indoleamine 2,3-dioxygenase expression by dendritic cells and subsequently impacts lymphocyte proliferation. Mem Inst Oswaldo Cruz **109,** 70, 2014.
52. Wang, J., Wang, Y., Wang, S., *et al.* Bone marrow-derived mesenchymal stem cell-secreted IL-8 promotes the angiogenesis and growth of colorectal cancer. Oncotarget **6,** 42825, 2015.
53. Opal, S.M., and DePalo, V.A. Anti-inflammatory cytokines. Chest **117,** 1162, 2000.
54. Xing, Z., Gauldie, J., Cox, G., *et al.* IL-6 is an antiinflammatory cytokine required for controlling local or systemic acute inflammatory responses. J Clin Invest **101,** 311, 1998.
55. Li, P., Li, S.H., Wu, J., *et al.* Interleukin-6 downregulation with mesenchymal stem cell differentiation results in loss of immunoprivilege. J Cell Mol Med **17,** 1136, 2013.
56. Giancola, R., Bonfini, T., and Iacone, A. Cell therapy: cGMP facilities and manufacturing. Muscles Ligaments Tendons J **2,** 243, 2012.

Address correspondence to:
Mohamed T. Ghorbel, PhD
Bristol Medical School
Bristol Heart Institute
University of Bristol
Research Level 7
Bristol Royal Infirmary
Marlborough Street
Bristol BS2 8HW
United Kingdom

E-mail: m.ghorbel@bristol.ac.uk

Received: June 12, 2017
Accepted: October 9, 2017
Online Publication Date: November 29, 2017